POSITION TRACKING CONTROL OF DC MOTOR FOR FRONT WHEEL SYSTEMS VIA HILS SIMULATION METHOD

M. F. A. Aili[1], F. Ahmad[1], M.H. Che Hasan[2], M. H. Harun[3] and M.H. Harun[1]

[1]Fakulti Kejuruteraan Mekanikal, Universiti Teknikal Malaysia Melaka, Hang Tuah Jaya, 76100 Durian Tunggal, Melaka, Malaysia

[2]Fakulti Teknologi Kejuruteraan Elektrik dan Elektronik, Universiti Teknikal Malaysia Melaka, Hang Tuah Jaya, 76100 Durian Tunggal, Melaka, Malaysia

[3]Fakulti Teknologi Kejuruteraan Mekanikal dan Pembuatan, Universiti Teknikal Malaysia Melaka, Hang Tuah Jaya, 76100 Durian Tunggal, Melaka, Malaysia

Corresponding Author's Email: faiq2711.aiman@gmail.com

Article History: Received 16 January 2023; Revised 16 February 2023; Accepted 13 March 2023

ABSTRACT: *This paper present about position tracking control of DC motor to be used as the actuator controller for the front wheel test rig system. The controller strategy that was developed is based on Proportional-Integral-Derivative (PID) controller. It consists of one single closed control loops namely position tracking control loop. To evaluate the effectiveness of the proposed controller, simulation and experimental studies were performed by using various input demand such as saw tooth, sine and step functions in 5°, 10°, 15° and 20° with the present of steering ratio at 360:20. The results, it is found that the trend between simulation and experimental data are similar with the command position with acceptable level of error which less than 10% for application at hand.*

KEYWORDS: *DC Motor; Position Tracking Control; HiLS Simulation; PID Controller; Front Wheel Test Rig*

1.0 INTRODUCTION

DC motors are extensively employed in a variety of settings, from industrial to home. They offer great torque and speed control, are dependable, and have a straightforward design. Position tracking is a key component in achieving accurate and effective control of DC motors. A system's capacity to precisely track and follow a desired position is referred to as position tracking control. The development of position tracking control algorithms for DC motors is the main topic of this research article. The goal is to give a thorough overview of the methods now in use and how well they work for precise and effective control of DC motors. In this study, DC motor mathematical models, position tracking control techniques, and performance evaluation through simulation and experimentation are all covered. The objective is to offer guidelines for future research in this field and insights into the design and implementation of position tracking control systems for DC motors.

The invention of the steer-by-wire system (SBW) [1], [2] was one of the systems in the automotive industry that was influenced by this technology. Steer-by-wire systems [3] and vehicle steering systems have recently evolved from pure mechanical generation to include hydraulic power-assisted steering (HPS), electrohydraulic power-assisted steering (EHPS), electric power-assisted steering (EPS), and finally steer-by-wire systems [4][5]. SBW used a high-performance dc motor to control the position of the wheel turning angle [6,7]. As a result, electronic components are required in the steering system, particularly for controlling the electric motor. The work of designing proper placement by the motor is vital and complex since the SBW movement is actuated by the motor. An adequate control strategy must be established as well as the requisite turning power needed to stop a wheel. Failure to do so will result in poor steering, which could result in an accident [8]. As a result, early in the SBW design process, a thorough investigation of the position tracking control of a dc motor is required.

Aside from that, the controller has already been demonstrated to be useful in a variety of applications. Simulations were run in MATLAB/Simulink software for various required inputs, including step, sine, and saw tooth functions with magnitudes of 5°,10°,15°and 20° to assess the performance of the controller structure. Extensive validations tests were carried out using the hardware-in-the-loop-simulation (HILS) technique to verify the controller's efficiency in a real-world environment. The validation's goal is to see if the control method is suitable for its intended use over the entire area of its applicability.

2.0 METHODOLOGY

2.1 Model and Simulation

Figure 1 shows the schematic diagram of DC motor that was used in this research. The DC motor converts electrical energy into mechanical energy which produced the torque needed to move the load to the desired output position $\tau(t)$ or rotate at the specified output angular speed $\omega_r(t)$. The generated torque is used to accelerate the rotor, and this mechanical power is eventually transmitted to the steering rack and the front wheel.

As a result, a portion of the torque will cause rotational acceleration of the rotor due to its inertia, J_{dc}, and the remaining energy will be dissipated in the bearings due to viscous friction, B_m and rotational speed. Below is the DC motor's mathematical equation found in [9].

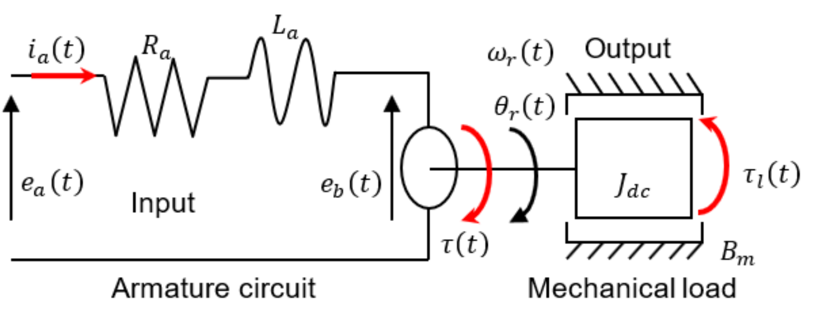

Figure 1: Schematic diagram of DC motor

The armature circuits

$$e_a(t) = R_a i_a(t) + L_a \frac{di_a(t)}{dt} + e_b(t) \tag{1}$$

The connections between mechanical and electric parts are described as:

$$\tau(t) = K_\tau i_a(t) \tag{1}$$

$$e_b(t) = K_b \omega_r(t) \tag{2}$$

By considering the mechanical load, the rotational acceleration of the DC motor shaft is described as:

$$J_{dc}\ddot{\theta_r}(t) = \tau(t) - B_m\dot{\theta_r}(t) - \tau_l(t) \tag{3}$$

The rotor angular speed is obtained by integrating the rotational acceleration as shown as follow:

$$\omega_r(t) = \dot{\theta}_r(t) \tag{4}$$

The front axle motor torque was selected since it is proportionate to a range of loads. When coupled to the front axle DC motor, the rack and pinion system is affected by the response torque of the load. As a result, the front axle motor torque always varies with the load. As a result, any changes to the load will have an immediate impact on the torque of the front axle motor. The current measurement method is employed to calculate the torque at the front axle motor.

The direct corresponding torque to the current of the motor is defined by Roland et al. [137]. Thus, the front axle motor torque is consisted for the front axle motor constant and the motor current is written as follows as shown in equation 6, the input from the torque produce by motor at front wheel and transmitted it into steering wheel torque driver and produced the output torque;

$$T_{fm} = i_{a2}k_{fm} \tag{5}$$

2.2 PID Controller Design

To achieve and sustain the process set point, one of the most often used controllers, PID control [10]-[15], can be utilized. PID control applications can differ, but the general strategy is always the same. The following is the PID controller equation in ideal parallel form:

$$u(t) = K_p * e(t) + K_i \int_0^t e(t)de(t) + K_d \frac{de(t)}{dt} \tag{6}$$

Where k_p is a constant variable for proportional gain, k_i is a constant variable for integral strengthening, k_d is a constant variable for derivative gain, *e(t)* is a variable for the error value and *u(t)* is a variable for control signals. k_p, k_i and k_d are control constant variables which have nonnegative values.

The variable k_p is employed in proportional control as an amplification, which can decrease rise time but generate and increase error [15] – [19]. Although the integral control uses the variable k_i to eliminate steady-state mistakes, it has the potential to exacerbate abrupt responses. To increase system stability, lessen overshoot, and enhance transient response, derivative control employs the k_d variable. PID control is implemented and simulated using PID blocks in Simulink MATLAB. Figure 2 and Table 1 display each block diagram's key components and the function of it. Using the experimental method of PID parameter enhancement, the controller settings were changed.

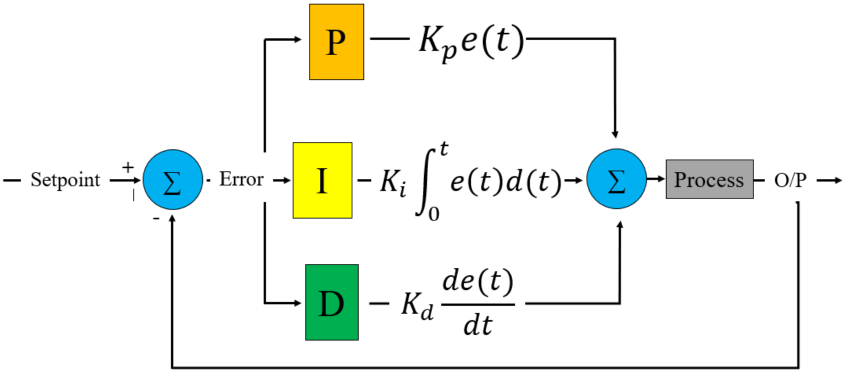

Figure 2: The designed PID controller in Simulink

Table 1: Characteristic of PID controller

Parameter	Rise time	Overshoot	Settling time	Steady-state error
k_p	Decrease	Increase	Small change	Decrease
k_i	Decrease	Increase	Increase	Eliminate
k_d	Small change	Decrease	Decrease	Small change

2.3 DC Motor Controller

There are two sets of closed loops use to compare between the simulation closed loop and closed loop for the hardware test rig. The reference input to the control system is the desired position angle, θ while the output of the control system is the actual position that produce from the steering rack as shown in Figure 3. The PID parameters of the controllers were tuned by using Ziegler's Nichols method and shown in Table 2.

Table 2: Controller parameters

Controller	P	I	D
Simulation	45.5	0.2	13
Experiment Test Rig	0.056	-	-

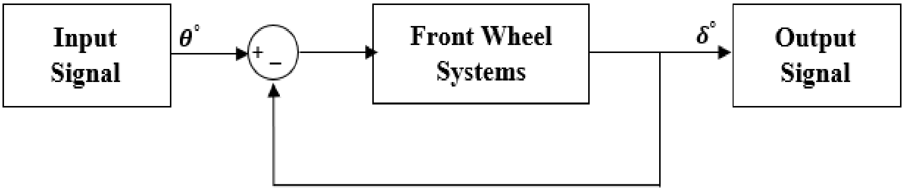

Figure 3: Control structure of DC motor

2.4 Front Wheel Test Rig

Due to the removal of the mechanical connection between the steering wheel and front wheel components, both test rigs are now separate and will be used to represent the system's actual use. Next, in Figures 4 illustrate the test rig for the front wheel system which contains of DC motor, encoder sensor, potentiometer and steering rack. This test rig is use to track if the DC motor will turn the steering rack and follows the input signal from the simulation software of MATLAB/Simulink.

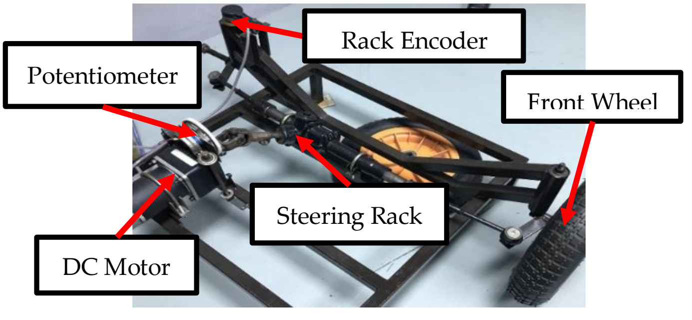

Figure 4: Front Wheel System Test Rig

2.5 Experimental Setup for HiLS

Figure 5 shows the hardware-in-the-loops simulation (HiLS) setup for position tracking of DC motor. It includes a Front Wheel test rig, a potentiometer, Motor Driver MD10C, National Instrument (NI) SCB 68 PCI 6251 and Host PC. The potentiometer is used to sense the rotational output from the rotor, while the Motor Driver MD10C is used as the motor driver. The communication and current control of the DC motor are made by using NI SCB 68 PCI 6251and NI card place in the target PC.

HiLS is the one of validation and comparison process for an experiment project. HiLS is a combination of experiment and simulation where for this paper, the HiLS process is done where the input signal will be obtained from the simulation received from MATLAB/Simulink software while the output will be visible on the front wheel test rig [20]. In other hand, all the results can also be found in the simulation where they are obtained from the readings of the encoder sensor that is attached to the steering rack.

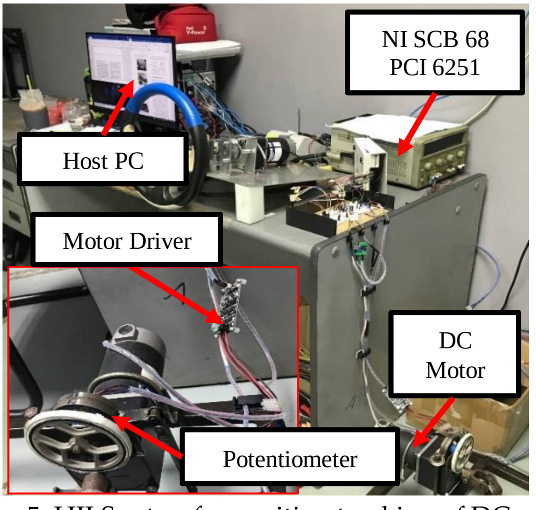

Figure 5: HILS setup for position tracking of DC motor

3.0 RESULTS AND DISCUSSION

Figures 6 to 8 shows the performances of position tracking control of the DC motor at front wheel test rig in various desired inputs of 5°, 10°, 15° and 20° due to the steering ratio of 360:20 [21] and the maximum of steering rack to turns are at 20°. In all figures, the dotted lines represent the input signals to the controller, the dot-dashed lines represent the simulation responses and the solid lines characterize the experimental responses. Based on the results from Figure 6, it can be said that the position tracking response shows a good agreement at the end of the response between desired trajectories with the actual response from simulation and experimental data but there is delay because of the mechanical part and the frictional force that been neglected in simulation software.

However, in Figure 6 there are delay in rise time occur in experimental results as compared to the desired position, the mean absolute value for experiment rise time is at 2.1s while the simulation's rise time is at 2s same with the input signal. Otherwise, in term of percentages of overshoot, the mean absolute value for experiment is 11.65%. Aside from that, the position tracking on sinusoid function at various peak positions show a very good tracking performances in both simulation and experimental results. There are depicted in Figure 7.

For position tracking using saw-tooth function with various peak forces is shown in Figure 8. It can be seen that in this function, the position tracking system is in good performance although it is rather difficult to closely follow the desired position especially at the peak position. As for the experiments, there are two values percentages that are at earlier peak and percentages value for the peak after. The mean absolute percentages for peak angle value at simulation is 6.865% less than the reference peak angle. Peak angle values for earlier and later peaks had mean absolute percentages that are, respectively, 11.745% and 14.598% smaller than the reference peak. This demonstrates that although the experiment's results produced a smaller peak, the signal still closely resembled the reference signal. This may be the result of the mechanical component's backlash and frictional force being ignored by the simulation software.

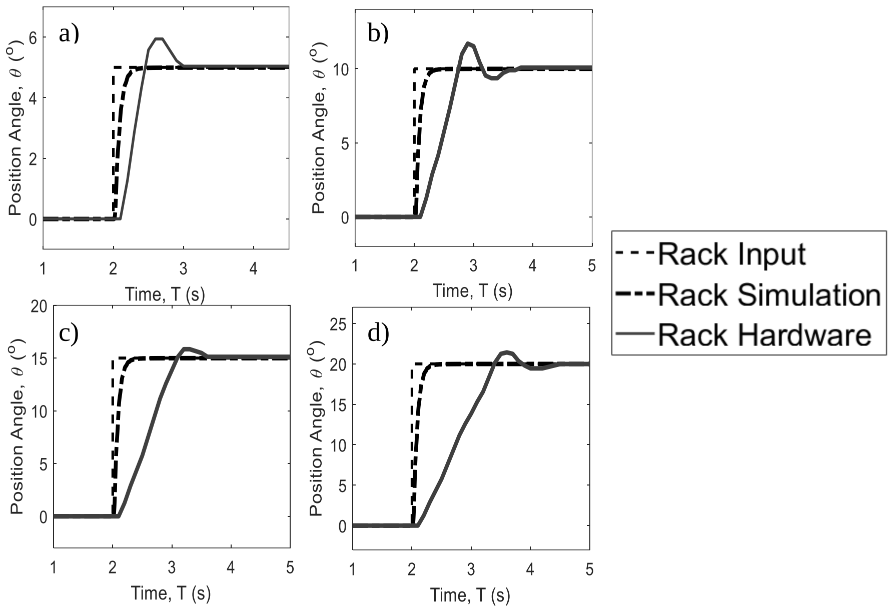

Figure 6: Responses of position tracking control for step function for; a) 5°, b) 10°, c) 15° and d) 20°

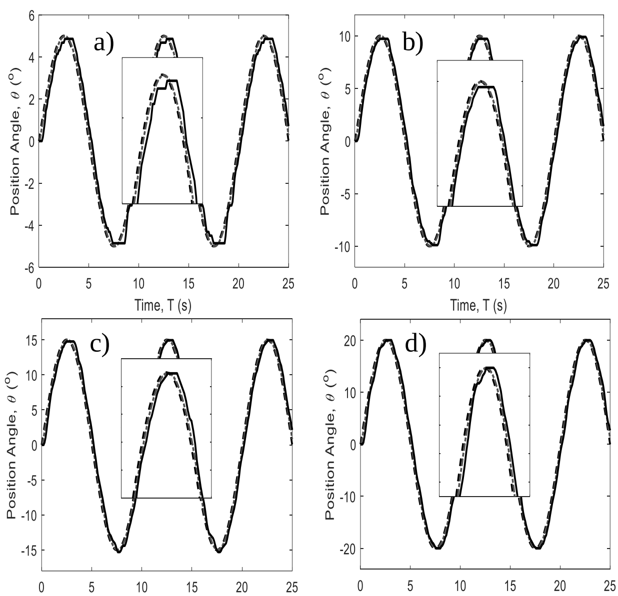

Figure 7: Responses of position tracking control in sine function for; a) 5°, b) 10°, c) 15° and d) 20°

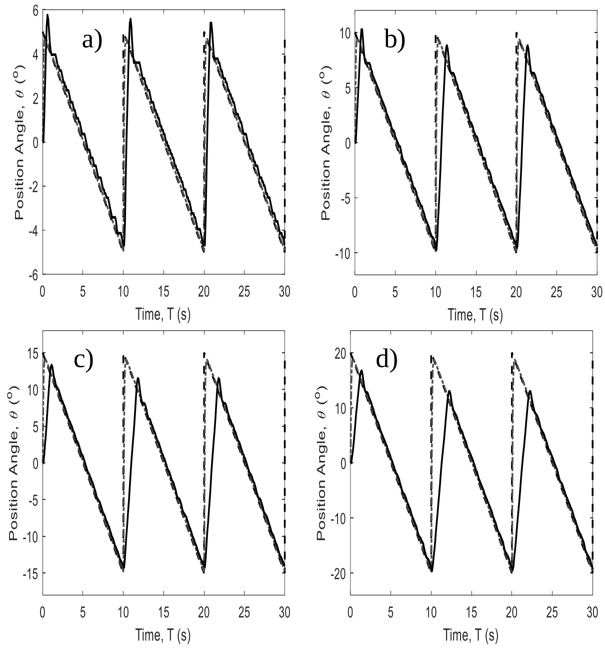

Figure 8: Responses of position tracking control in saw tooth function for a) 5°, b) 10°, c) 15° and d) 20°

From those results, it can be concluded that the performance of position tracking control of DC motor in three signals of continuous and discontinuous functions are moderately good. The weakness of the proposed position control is seen at the discontinuous function such as step functions and saw-tooth functions due to the incapability of system to follow the rapid change of the target position. However, at the typical continuous function such as sinusoid function, the position tracking control is excellent. The deviation between simulation and the experimental results may be due to the backlash between the potentiometer shaft and the motor shaft that delaying the system responses.

4.0 CONCLUSION

In this study, a position tracking control of DC motor based PID controller has been developed. It consists of one single closed loop which act as the position controller to the DC motor. In order to verify the effectiveness of the controller strategy, several tests were conducted through simulation and experimental studies. The tests used were position input demand at 5°, 10°, 15° and 20° due to steering ratio of 360:20 in step, sine-wave and saw tooth function respectively.

From the results, it can be said that the behavior of the simulation and the experimental data are almost similar as the command position with minor deviation particularly in step and saw tooth function. It also noticed that the ability of the controller system in mocking up the command position is very promising. However, there is delay in the rise time on the experimental data as compared to the command position with average delay up to 2.1s while the simulation's rise time same as the input command signal. The delay in the experimental data is because of the slip between gear at potentiometer shaft and the at the rotor shaft. Nevertheless, it can be concluded, the potential benefit of the controller strategy to the system was found to be effective and ready for the application at hand.

ACKNOWLEDGMENTS

This work is a part of a research projects entitled "Torque Vectoring Based Direct Yaw Moment Control of Electric Vehicle Using Individually Actuated in-wheeled Motors", funded by PJP grant (PJP/2022/FTKMP/S01888) and continuation from the previous research project "Characterization of brake force and wedge properties of IBS based electronic wedge brake for autonomous braking system", grant no. (PJP/2020/FKM/PP/S01783) lead by Ir. Ts. Dr. Fauzi Ahmad. The authors would like to acknowledge support from Universiti Teknikal Malaysia Melaka for providing the research facilities.

REFERENCES

[1] J. Kim, C. Jo, Y. Kwon, J.S Cheon, S.J Park, G. Jeon and B. Shim, "Electromechanical brake for front wheel with backup braking". *SAE International Journal of Passenger cars – Mechanical System*, vol. 7, no.4, pp. 1369-1373, 2014.

[2] S. Haggag and D. Abidou. An approach to vehicle brake-by-wire optimal control tracking strategy. *SAE International Journal of Passenger Cars – Mechanical System*, vol.6, no. 1, pp. 154-162, 2013.

[3] M.L.H Abd. Rahman, K. Hudha, F. Ahmad and H. Jamaludin. Design and clamping force modeling of electronic wedge brake system for automotive application. *International Journal of Vehicle Modeling and Testing*,vol. 8, no.2, pp. 145-156, 2013.

[4] Robert Bosch GmbH, (2014), "Bosch automotive electrics and automotive electronics: Systems and components," in Networking and Hybrid Drive. Plochingen, Germany: Springer-Verlag.

[5] S. A. Arogeti, D. Wang, C. B. Low, and M. Yu. "Fault detection isolation and estimation in a vehicle steering system," *IEEE Trans.Ind. Electron.*, vol. 59, no. 12, pp. 4810–4820, 2012.

[6] V. R. Aparow, K. Hudha, F. Ahmad and H. Jamaluddin. Model in the loop simulation of gap and torque tracking control using electronic wedge brake, *International Journal of Vehicle Safety*, vol. 7, no.3/4, pp. 390 – 408, 2014.

[7] K. Han, M. Kim and K. Huh. Modeling and Control of an Electronic Wedge Brake. *Proceeding of the Institution of Mechanical Engineers, Part C: Journal of Mechanical Engineering Science*,vol. 226, no.10, pp. 2440-2455, 2012.

[8] M. A. A. Emam, A. S Emam, S. M El-Demerdash, S. M Shaban and M.A Mahmoud. Performance of Automotive Self-reinforcement Brake System. *Journal of Mechanical Engineering*, vol. 1, no.1, pp. 4–10, 2012.

[9] C. E Castaneda, D. Lopez-Mancilla, J.H Garcia, R.J Reategui, G. Huerta and R. C Zarate. Position Control of DC motor Based on Recurrent High Order Neural Networks. IEEE Proceeding on International Symposium on Intelligent Control, Part of 2010 IEEE Multi-Conference on Systems and Control. September 8-10, Yokohama, Japan, pp.1-6, 2010.

[10] M. Ren, J. Zhang, H. Yue, and S. Zhou, "Adaptive neural network cascade control system with entropy-based design," *IET Control Theory Appl.*, vol. 10, no.10, pp. 1151–1160, 2016.

[11] C. Jauregui, M. Duarte Mermoud, G. Lefranc, R. Orostica, J. C. Travieso Torres, and O. Beytia, "Conical Tank Level Control with Fractional PID," *IEEE Lat. Am. Trans.*, vol. 14, no.6, pp. 2598–2604, 2016.

[12] A. S. Bazanella, L. F. A. Pereira, and A. Parraga, "A New Method for PID Tuning Including Plants Without Ultimate Frequency," *IEEE Trans. Control Syst. Technol.*, vol. 25, no. 2, pp. 637–644, 2017.

[13] J. Fei, Y. Chu, and S. Hou, "A Backstepping Neural Global Sliding Mode Control Using Fuzzy Approximator for Three-Phase Active Power Filter," *IEEE Access*, vol. 5, pp. 16021–16032, 2017.

[14] J.-H. Yang and H.-K. Xu, "Robust Controller Design for NonMinimum Phase UAV System and System Analysis," *IEEE Access*, vol. 6, pp. 70734–70769, 2018.

[15] A. Bisoffi, M. Da Lio, A. R. Teel, and L. Zaccarian, "Global Asymptotic Stability of a PID Control System with Coulomb Friction," *IEEE Trans. Automatic Control*, vol. 63, no.8, pp. 2654–2661, 2018.

[16] S. Han and S. P. Bhattacharyya, "PID Controller Synthesis Using a -Hurwitz Stability Criterion," *IEEE Control Syst. Lett.*, vol. 2, no. 3, pp. 525–530, 2018.

[17] J. Wang, Z. Luo, Y. Wang, B. Yang, and F. Assadian, "Coordination Control of Differential Drive Assist Steering and Vehicle Stability Control for Four-Wheel-Independent-Drive EV," *IEEE Trans. Veh. Technol.*, vol. 67, no.12, pp. 11453–11467, 2018.

[18] T. MohammadRidha, "Model Free iPID Control for Glycemia Regulation of Type-1 Diabetes," I*EEE Trans. Biomed. Eng.*, vol. 65, no. 1, pp. 199–206, 2018.

[19] V. Gholamrezaie, M. G. Dozein, H. Monsef, and B. Wu, "An Optimal Frequency Control Method Through a Dynamic Load Frequency Control (LFC) Model Incorporating Wind Farm," *IEEE Syst. J.*, vol. 12, no. 1, pp. 392–401, 2018.

[20] M.Z Amir and M.F Abd Samad, "Hardware-in-the-loop simulation of steer-by-wire system in automotive vehicle" International Journal of Advanced and Applied Sciences, vol. 3, no.9, pp. 51-58, 2016.

[21] R. Jadoun and C. Sushil. "Design and fabrication of variable steering ratio mechanism for light Motor vehicle". *Innovative system Design & Engineering*, vol. 5, pp. 7-15, 2014.